Low Complexity Image Quality Measures for Dietary Assessment Using Mobile Devices

Chang Xu*, Nitin Khanna*, Carol J. Boushey† and Edward J. Delp*
*School of Electrical and Computer Engineering Purdue University
West Lafayette, Indiana, USA
†Epidemiology Program, University of Hawaii Cancer Center
Honolulu, HI, USA

***Abstract*—Many chronic diseases, such as heart disease, diabetes, and obesity, can be related to diet. Hence, the need to accurately measure diet becomes imperative. We are developing image analysis tools for the identification and quantification of foods consumed at a meal. Our system relies on a single meal image from the user for doing food identification and quantity estimation. Therefore, it is very important to assist the user in acquiring a good quality image by providing immediate feedback about the image quality. This paper presents low complexity image quality measures which are deployed on handheld mobile devices.**

I. Introduction

There is a growing concern in the world about chronic diseases related to diet, including obesity, cancer, diabetes, and heart disease. Of the 10 leading causes of death in the U.S., 6 are related to diet. Collection of food intake and dietary information provides valuable insights into the occurrences of diseases and subsequent approaches for mounting intervention programs for prevention. However, accurate assessment of diet is problematic, especially in adolescents [1]. The assessment of food intake in adolescents has been evaluated by food records, the 24-hour dietary recall, and food frequency questionnaire with external validation by doubly labeled water (DLW) and urinary nitrogen. The consistent finding of underreporting is a major drawback of these dietary assessment methods [1], [2]. Accurately measuring dietary intake is considered to be an open research problem in the nutrition and health fields. Dietary assessment methods perceived as less burdensome and less time-consuming may improve compliance [3]. The use of a mobile telephone's built-in digital camera has been shown to provide unique mechanisms for reducing user burden and improving the accuracy and reliability of dietary assessment [4].

An on line food-logging system is presented in [5], which distinguishes food images from other images, analyzes the food balance, and visualizes the log. Global and local features are used to describe food items and classify them using a Support Vector Machine (SVM). This system aims to estimate calories and nutrient values of a meal by classifying different food items into broad categories such as grains, vegetables and so on. A food intake visual and voice recognition (FIVR) system is presented in [6]. This system obtains a set of three images of user's plate of food, along with a list of food items through speech. It then uses classifiers trained between all pairs of foods to recognize food types, estimates their volumes and finally returns quantitative nutrition information. In [7], a multiple kernel learning method is presented to integrate color, texture, and SIFT descriptors for food identification. A single feature vector is formed by combining these three classes of features with different weights. In [8] a method for food identification is presented that utilizes the spatial relationship among different ingredients (such as meat and bread in a sandwich). The food items are represented by pairwise statistics between local features of the different ingredients of the food items.

We are developing a system, known as the mobile device food record (mdFR), to automatically identify and quantify foods and beverages consumed by analyzing meal images captured with a handheld mobile device [9], [10].

One of the original methods of using digital images to collect food intake involves school children handing their tray to an individual for placement in a standardized holder for image capture [11]. In general, one tray of food is weighed, imaged, and used as a reference for estimating portions on all of the trays [11]. The method is cumbersome with respect to the number of staff involved, however the results have been satisfactory with regard to a trained analyst estimating amount of food consumed. One of the limitations is the inability to measure lunches brought from home due to the lack of a reference tray. The mdFR we are developing makes use of a fiducial marker and other contextual information that eliminates this problem. In our system, all the meal images have a calibrated fiducial marker which is used for color correction, camera parameter estimation and 3D reconstruction from a single image. A fiducial marker is an object used in the field of view of the camera that appears in the acquired image. It is used as a point of reference, a measure for camera calibration, and color correction. In our studies it is a small (7×6 cm^2) color checkerboard (Figure 1). Different user studies conducted at Department of Food and Nutrition, Purdue University, have shown that this fiducial marker is easy

This work was sponsored by grants from the National Institutes of Health under grants NIDDK 1R01DK073711-01A1 and NCI 1U01CA130784-01. Any opinions, findings, and conclusions or recommendations expressed in this material are those of the author(s) and do not necessarily reflect the views of the National Institutes of Health. Address all correspondence to Edward J. Delp, ace@ecn.purdue.edu or see www.tadaproject.org.

978-0-7695-4589-9 2011

DOI 10.1109/ISM.2011.64

to use with acceptable user burden. After using the mdFR, 65 of 71 adolescents (92%) responded that the fiducial marker would be easy to carry and use [12]. Adults have responded similarly [13]. Therefore, the mdFR can accommodate a wider gamut of eating conditions. Figure 1 shows an overview of our system [9], [10]. The first step is to send the image and metadata to the server for Image segmentation, food identification and volume estimation (step 2 and 3). These results are then sent back to the client where user confirms and/or adjusts this information (step 4). In step 5, the server receives the user confirmation and extracts the nutrient information using the FNDDS database (step 6). FNDDS is a database containing the most commonly eaten foods in the U.S., their nutrient values, and weights for different standardized food portions (step 6). Finally these results are sent to the research community for further analysis (step 7). Image segmentation, food identification, and volume estimation are the three main steps in automatic image analysis. Images captured before and after eating the foods are used to estimate the food intake. The energy of the food consumed can then be determined by using the density estimates for different food items. A complete description of the mdFR is presented in [9], [10]. A prototype of our system is deployed on the Apple iPhone as the client and has been used for different user studies at the Department of Food and Nutrition at Purdue University.

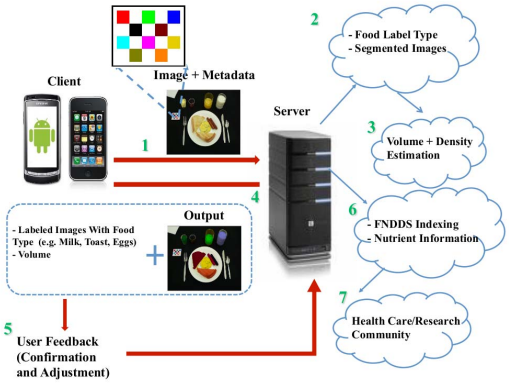

Fig. 1. Overall System for Dietary Assessment [9], [10].

Full utilization of the additional information provided by the use of a fiducial marker and other contextual informations is very important for dealing with the challenges involved in food classification and volume estimation from a single image. For instance, food identification is a difficult problem since foods can dramatically vary in appearance [14], [15]. Such variations may arise not only from non-rigid deformations, and intraclass variability in shape, texture, color and other visual properties, but also from changes in illumination and viewpoint. Color features play a very important role in food identification and many food items have closely related colors [14] while there is a wide range of illumination conditions for different eating occasions. Thus, color correction plays a crucial role in different dietary assessment methods [6], [9], [10]. Most of these methods use some kind of fiducial marker for estimating unknown illumination conditions and subsequently using different color correction methods for mapping the test image back to the reference illumination conditions. Similarly, the fiducial marker plays a key role in 3D reconstruction from a 2D image for estimating the volumes of different food items [6], [16]. Hence, integrating real-time image quality check on the mobile devices will result both in a better user experience with less user burden and in circumventing image analysis problems due to images of inadequate quality.

This paper concentrates on low complexity image quality assessment methods for dietary assessment using mobile devices. Our goal is to detect the image quality issues before users save images of their meals and assist them in capturing better images. Apart from the general notion of image quality such as sharpness, in the context of dietary assessment, good quality images need to satisfy specific requirements such as the presence of a fiducial marker, appropriate camera angle and so on. Based on our user studies the most significant reasons for poor quality images are: non-detectable fiducial marker (forgetting to use the fiducial marker or overexposed/blurred images), spectral reflections, shadows, insufficient illumination, and blur. In this paper, we focus on fiducial marker detection and blur estimation. All the existing dietary assessment methods using mobile devices [6], [9], [10], [5], use them only as the front-end to capture meal images and to send them to back-end servers, using a graphical user interface. Computation intensive steps are performed on the network connected server. Performing image quality assessment on the servers and sending back the response to the user is not feasible in most of the circumstances, due to associated network and computation delays. Mobile devices have limited computation power and the image quality check needs to be performed before the image is saved. Therefore, these methods must use small computation and memory resources. Our methods have been deployed on the iPhone without adding any perceptible delay in the image capture step and thus enhances the user experience.

II. Fiducial Marker Detection

The problems encountered in designing the mobile device food record (mdFR) are fundamentally difficult; however it is possible to solve these problems by properly utilizing contextual information. For example, the fiducial marker provides a reference for camera calibration as well as color correction, and thus makes it feasible to use mdFR in a wider range of eating occasions. In our studies a small (7×6 cm^2) planar color checkerboard (Figure 1) is used as the fiducial marker and all the images captured by using our system contain this fiducial marker. A planar black and white checkerboard pattern with known geometry is widely used for camera calibration [17]. The alternating black and white grids produce the basic crossing feature points which make it easy to detect under varying imaging conditions.

In our system, we are interested in using the fiducial marker both for camera calibration (geometry reference) and color correction (color reference), thus we designed a color checkerboard to use as the fiducial marker. Since this fiducial marker is intended to be used with a mobile application, users need to carry these along with their phones. Therefore, the fiducial marker needs to be small, preferably credit card size and at the same time, it needs to be large enough to provide the geometry information. Presently, we are using a fiducial marker of size 7×6 cm^2, which typically corresponds to around 280×240 pixels in a 2048×1536 image captured using our application on the iPhone. Further, to provide enough information for good color correction, the fiducial marker should have a wide range of colors. Thus, we have chosen all three primary colors and some other frequently occurring colors for different squares on our fiducial marker (Figure 1). In the present version, it has ten different colors on a white background. It also has a black border around it to help in the quick identification step. These specific characteristics of our fiducial marker provide us more contextual information but they also prevent direct application of traditional methods for checker board detection [18], [19], [20].

In [21], [22] checkerboard detection is done by finding the edges and fitting lines to them. The corners are detected as the intersection of straight lines fitted to each square. This method works well for high contrast images captured under good illumination. But under insufficient illumination, it may not find the entire checkerboard. Another approach is to directly detect the corners of the checkerboard. Existing checkerboard corner detection methods [23], [24] generally use a refined Harris or Susan corner finder to locate all possible corner points, and then apply some distance or neighbor constraints to group the corners. This step is followed by matching the checkerboard pattern. However, existing methods for checkerboard marker detection often fail for our color checkerboard, as the colored design possesses less contrast (such as yellow color on white background, under yellow light) than the black and white version. In addition, most of these methods use a global adaptive threshold for converting a gray-level version of a color image to a binary image, thus the brightness of the image can affect the ability of these methods to recognize the corners or the lines. Therefore a robust method for color checkerboard detection in unconstrained environments is required.

For the images captured using our application to be useful for further image analysis, we need to automatically detect the presence of the fiducial marker. These methods need to be implemented on the mobile device and provide immediate feedback before saving the image. Compared with traditional methods, the proposed approach reduces the time cost for searching the corners, speeds up image preprocessing and adapts to automatic image quality assessment on mobile devices. To achieve this, we make suitable modifications in existing methods [25] by utilizing special characteristics of our fiducial marker such as the black border around it. The proposed approach for checkerboard pattern detection is based on a region search method, which is less sensitive to illumination changes and noise. It consists of two steps, the first step is to detect possible candidate regions for the presence of the fiducial marker and the second step is to identify the checkerboard pattern and find corners of each color patch.

A. Candidate Region Detection

One of the distinctive characteristics of our fiducial marker is that it has a black border on a white background. Thus, any quadrilateral region enclosed by a black border is a possible candidate region. Black borders can be easily identified in a binary image obtained by applying a global adaptive threshold to the color image. Initial denoising is done by using a Gaussian filter. Then, a fixed global threshold is used on the gray scale version of the colored, denoised meal image. After connected component analysis on black pixels of the binarized image, we need to reject the components with very small areas. For a meal image to have sufficient resolution for automatic dietary assessment, the area of the fiducial marker region should be neither too large nor too small. Thus from the connected components obtained by using black pixels, we reject those regions which have areas (number of pixels) smaller than 1% or larger than 9% of the total number of pixels in the image. Among the regions satisfying the size criteria, we need to select those regions which can be well approximated by a quadrilateral. This step is done by using the Douglas-Peucker(DP) method [26] for estimating a contour from a sequence of points. It finds the minimum number of dominant points (corners of a polygon) that represent a polygon approximation to the contour. In our implementation, we first look for two boundary points on the contour with the largest mutual Equlidean distance and connect them with a line. Then, we find another dominant point with the largest distance from this line, and if the distance is larger than a precision threshold, we add it into the approximation. The algorithm recursively finds the next most distant point until it converges to a good approximation of the contour. Alternatively it finds the fifth dominant point since we are only interested in polygons with four points as candidate regions for the fiducial marker.

B. Internal Corners Estimation Using Quadrangles

After finding the candidate regions, the next step is checkerboard matching by detecting the internal corners. This is a three step process consisting of quadrangle generation, quadrangle grouping and corner estimation. This series of operations is independently performed on each of the candidate regions of interest.

1) Quadrangle Generation: The first step is to obtain a binary version of the color patch corresponding to the candidate region of interest. This cannot be done by using the global threshold used in the previous step, because our fiducial marker contains low contrast boundaries such as a yellow square on a white background. Instead, we estimate the background color (for the checkerboard region and not for the entire image) as the most frequently occurring graylevel in the histogram for the candidate region of interest. Then, the binary

image is obtained by assigning 1 to all the background pixels and 0 to rest of the pixels. This procedure will allow us to separate background pixels from the color patches even if they differ by a small amount. Next, a dilation morphological is applied to the binarized version of the candidate region. In this way, we separate the connected area between checkerboard patches and obtain a group of quadrangles.

2) Quadrangle Grouping: Groups of quadrangles are found using their position and neighborhood relation with respect to other quadrangles. Neighboring quadrangles are estimated according to the distance to every corner of every other quadrangle. The smallest of such distances are stored along with the respective corner and quadrangle ID.

3) Corner Estimation: Finally, the groups of quadrangles obtained above are compared with the connected quadrangles of desired pattern. The connected quadrangles set, which has the same property as our checkerboard pattern is declared as the checkerboard region. And the four dominant points of these quadrangles obtained from DP method are the external corners of the fiducial marker, while the corners of each of the constituent quadrangles give us the internal corners of the fiducial marker.

III. Blur Detection

Blur is one of the most frequent causes of image distortion. Image blur may be caused by a number of factors, such as out of focus blur, motion blur and loss of high frequency data during acquisition, compression or processing. Out of focus blur results from an incorrect focus of the entire or part of the image and is frequently modeled by convolution with a Gaussian kernel. Motion blur results from relative motion between the camera and the objects during exposure and is modeled by attenuating specific coefficients in the frequency domain.

Blur has considerable influence on food identification and quantification using digital images. It is obvious that a high degree of blur can change the edge structure of an image, resulting in wrong segmentation due to missing boundaries and wrong classification due to changes in appearance of foods, especially the texture features. For object classification, some features, such as an RGB color histogram, are robust to a smoothing effect due to blur. However, some descriptors, mostly edge-based descriptors such as SIFT, are extremely sensitive to blur.

Several experiments, using both user-taken blurred images and simulated blurred images, are performed to quantify the effect of blur on image analysis steps of our proposed dietary assessment method. In one of these experiments, linear motion blur is applied to thirty food items. Linear motion blur is generally modeled as a convolution (Equation 1) and is characterized by two parameters, L which represents motion length and ϕ which denotes motion direction. The effect of motion blur is evaluated on the widely used SIFT features [27]. SIFT descriptors of an original food image are matched with those corresponding to different distorted images generated by applying linear motion blur with different kernel lengths L and blur angles ϕ. The descriptor's accuracy is estimated by counting the percentage of SIFT points from the original image that could be matched to the SIFT points of the distorted image. Figure 2 shows the results of one such experiment where the curve consisting of diamond symbols indicates that the matching accuracy of SIFT descriptors quickly drops with the increase in motion blur. Hence, for successful food identification, its important to eliminate the image quality degradation due to blur.

$$h(x,y) = \begin{cases} \frac{1}{L} & \text{if } \sqrt{x^2+y^2} \leq L \text{ and } \frac{y}{x} = tan(\phi) \\ 0 & otherwise \end{cases} \quad (1)$$

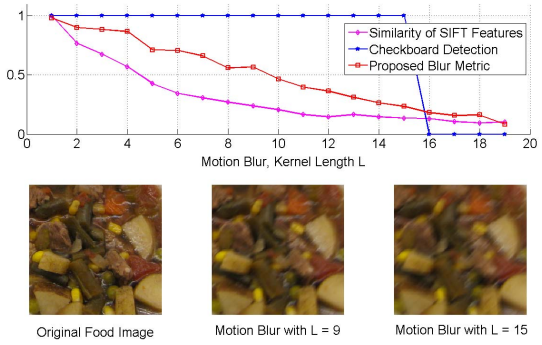

Fig. 2. Effect of Image Blur on SIFT Features and Proposed Blur Metric.

In our application, problems due to blur can be alleviated by either restoring the blurred image by post-processing or obtaining a blur assessment on the mobile device and if needed retaking the image. A number of methods have been proposed to restore blurred images [28], [29], [30]. However, there is no guarantee that even the best restoration method will be able to recover all the useful information from a degraded image. Further, blur restoration methods may take lot of computation and may result in other distortions such as ringing. Therefore, for our application it is more practical to perform real-time blur estimation on the mobile device and if needed, prompt the user to retake the image.

A. Related Work

Most of the existing blur assessment methods can be classified into two categories: frequency domain methods and spatial domain methods. Frequency domain methods estimate the blur level of an image by utilizing the observation that blur could be caused by attenuation in the high-frequency coefficients. For example, distribution of null DCT coefficients can be used for blur assessment [31]. Coefficients on the central diagonal of DCT matrix are used for this purpose since they are good representatives of the global blur and their histogram provides a blur metric. Spatial domain methods focus on the "appearance" (e.g. edge and gradient) of an image in spatial domain. Mariliano et al. [32] proposed that the smoothening effect of blur on sharp edges can be used as an indicator of

blur and the spread of edges can be used as a blur metric. Generally, spatial domain methods are more efficient than the frequency domain methods as they do not require an additional transformation to another domain. In this paper, we present a low complexity blur metric by doing suitable modifications to a well known method called cumulative probability of blur detection (CPBD) which utilizes probability distribution of edge widths [33].

In [33], a no-reference blur metric is proposed that combines the edge width method [32] and the concept of "just noticeable blur." Blur metric estimation begins with applying a Sobel operator in the vertical direction on the luminance component of the image. An edge binary map is constructed to indicate the location of points where the gradient magnitude assumes a local maximum in the vertical direction. Since the smooth areas have little influence on blur estimation, the image is divided into 64×64 blocks to determine the regions of interest. The blocks containing a number of edge points larger than a fixed threshold are considered as edge blocks. At each edge pixel within the edge blocks, edge width is estimated as the distance between the start and end of local extrema [32]. Let e_i denote an edge pixel and $\omega(e_i)$ its corresponding edge width. Then, the probability of blur detection P_{BLUR} at each edge pixel can be expressed in the following form [33]:

$$P_{BLUR}(e_i) = 1 - exp\left(-\left|\frac{\omega(e_i)}{\omega_{JNB}(e_i)}\right|^{\beta}\right). \quad (2)$$

where β is a value chosen between 3.4 and 3.8 with a mean value of 3.6 and JNB width $\omega_{JNB}(e_i)$ depends on the local contrast C of the edge block corresponding to edge pixel e_i.

Finally, the overall blur metric, cumulative probability of blur detection (CPBD) is estimated as:

$$CPBD = P(P_{BLUR} \leq P_{JNB}) = \sum_{0}^{P_{JNB}} P(P_{BLUR}) \quad (3)$$

where $P(P_{BLUR})$ denotes the value of probability distribution function at a given P_{BLUR} [33].

B. Proposed Method

For deploying blur assessment method on a mobile device, it needs to have low computation and memory requirements. This section describes our modifications to CPBD method which result in reduction in its time complexity. The blur metric CPBD (Equation 3) can be represented as:

$$CPBD = \frac{|S_1|}{|S_e|}. \quad (4)$$

where S_e denotes the set that contains all the edge pixels, and S_1 donates the set of edge pixels with $P_{BLUR} \leq P_{JNB}$. Using Equation 2, this condition is same as:

$$1-\exp\left(-\left|\frac{\omega(e_i)}{\gamma}\right|^{\beta}\right) \leq 0.63 \Rightarrow \omega\left(e_i\right) \leq \gamma\times[-\ln\left(0.37\right)]^{\frac{1}{\beta}}, \quad (5)$$

where γ donates JNB width $\omega_{JNB}(e_i)$. Since the JNB width γ takes on only two values 5 and 3 when local contrast $C \leq 50$ and $C > 50$, respectively [33] (the local contrast C is obtained by subtracting minimum intensity from the maximum intensity within the same edge block). Therefore,

$$\gamma \times [-ln\left(0.37\right)]^{\frac{1}{\beta}} = \begin{cases} 5 \times 0.9984, & \text{if } C \leq 50 \\ 3 \times 0.9984 & \text{if } C > 50. \end{cases} \quad (6)$$

$$\Rightarrow \omega\left(e_i\right) \in \begin{cases} \{2,3,4\} & \text{if } C \leq 50 \\ \{2\} & \text{if } C > 50. \end{cases} \quad (7)$$

In the last step, we utilized the fact that $\omega\left(e_i\right)$ is an integer since it represents the edge width. Let $H(\gamma,k)$ denote the number of edge pixels with JNB width γ and edge width k. Then, Equation 4 can be described as:

$$CPBD = \frac{\sum\limits_{\gamma=\{3,5\}}\sum\limits_{k=2}^{\gamma-1} H(\gamma,k)}{|S_e|}. \quad (8)$$

Estimation and use of $H(\gamma,k)$ can efficiently performed by storing it as a 5×4 matrix and using the following steps:

Input: Gradient Mask and Edge Blocks
Output: $H(\gamma,k)$
Initialize each $H(\gamma,k)$ to zero.
foreach *Edge Block* W **do**
  $C \leftarrow$ Max(I_W) - Min(I_W) **if** $C \leq 50$ **then**
    $\gamma \leftarrow 5$
  else
    $\gamma \leftarrow 3$
  end
  foreach *Edge Pixel* $e_i \in W$ *such that* $w(e_i) < \gamma$ **do**
    $H(\gamma, w(e_i)) \leftarrow H(\gamma, w(e_i)) + 1$
  end
end

Edge width computation is also efficiently done by utilizing the need for edge widths only when they are less than γ (3 or 5) and larger edge widths need not be computed. The proposed method of blur metric assessment saves considerable time compared to the original method as it involves only simple additions and multiplication (for gradient estimation) and none of the exponentials (Equation 2) need to be computed.

IV. Results

The proposed methods for fiducial marker detection and blur estimation were deployed on Apple iPhone and were tested under different imaging conditions including various backgrounds, and with complex illumination conditions. For fiducial marker detection, the pattern matching process is performed within a small part of the image. Therefore, we save time spent on exhaustively searching for potential corners, as done in traditional methods [18], [19], [20]. Experiments with the version deployed on the iPhone show that our

method takes approximately 1 second to detect the fiducial marker and is 10 times faster than the widely used OpenCV implementation [25].

Our proposed blur metric was evaluated on images of thirty food items under different degrees of blur. Figure 2 shows that the blur metric follows the same trend as accuracy of matching SIFT descriptors. Other food items with textured appearance have similar trends for the blur metric and accuracy of SIFT descriptor matching and a threshold of 0.5 can be used on the blur metric for alerting the user to retake the image. Both the accuracy of SIFT descriptor matching and the blur metric remain almost constant for the food items without much texture such as milk. The average time cost of original CPBD method is reduced from 9 seconds to 1 second on the mobile device for images 2048×1536 sized images.

V. Conclusion

Measuring accurate dietary intake is an open research problem in the nutrition and health fields. To automatically identify and estimate portions of foods in a meal image, it is crucial to obtain good quality images which aid image analysis. This paper presents low complexity methods for fiducial marker detection and blur assessment on mobile devices. Future work will include methods for shadow detection and suitable metrics for illumination conditions which can lead to color consistency.

References

[1] M. B. E. Livingstone, P. J. Robson, and J. M. W. Wallace, "Issues in dietary intake assessment of children and adolescents," *British Journal of Nutrition*, vol. 92, pp. S213–S222, 2004.

[2] M. U. Waling and C. L. Larsson, "Energy intake of swedish overweight and obese children is underestimated using a diet history interview," *Journal of Nutrition*, vol. 139, no. 3, pp. 522–527, March 2009.

[3] M. Livingstone, A. Prentice, W. Coward, J. Strain, A. Black, P. Davies, C. Stewart, P. McKenna, and R. Whitehead, "Validation of estimates of energy intake by weighed dietary record and diet history in children and adolescents," *American Journal of Clinical Nutrition*, vol. 56, no. 1, pp. 29–35, July 1992.

[4] C. J. Boushey, D. A. Kerr, J. Wright, K. D. Lutes, D. S. Ebert, and E. J. Delp, "Use of technology in children's dietary assessment," *European Journal of Clinical Nutrition*, vol. 63, pp. S50–S57, 2009.

[5] K. Kitamura, T. Yamasaki, and K. Aizawa, "Foodlog: capture, analysis and retrieval of personal food images via web," *Proceedings of the ACM Workshop on Multimedia for Cooking and Eating Activities (CEA)*, New York, USA, November 2009, pp. 23–30.

[6] M. Puri, Z. Zhu, Q. Yu, A. Divakaran, and H. Sawhney, "Recognition and volume estimation of food intake using a mobile device," *Workshop on Applications of Computer Vision (WACV)*, December 2009, pp. 1 –8.

[7] T. Joutou and K. Yanai, "A food image recognition system with multiple kernel learning," *Proceedings of International Conference on Image Processing (ICIP)*, Beijing, China, October 2009.

[8] S. Yang, M. Chen, D. Pomerleau, and R. Sukhankar, "Food recognition using statistics of pairwise local features," *Proceedings of International Conference on Computer Vision and Pattern Recognition (CVPR)*, San Francisco, CA, June 2010.

[9] F. Zhu, M. Bosch, I. Woo, S. Kim, C. J. Boushey, D. S. Ebert, and E. J. Delp, "The use of mobile devices in aiding dietary assessment and evaluation," *IEEE Journal of Selected Topics in Signal Processing*, vol. 4, no. 4, pp. 756–766, August 2010.

[10] N. Khanna, C. J. Boushey, D. Kerr, M. Okos, D. S. Ebert, and E. J. Delp, "An overview of the technology assisted dietary assessment project at purdue university," *Proceedings of the IEEE International Symposium on Multimedia*, Taichung, Taiwan, December 2010, pp. 290–295.

[11] S. M, "Digital photography as a tool to measure school cafeteria consumption," *Journal of School Health*, vol. 78, no. 8, pp. 432–437, August 2008.

[12] B. Six, T. Schap, F. Zhu, A. Mariappan, M. Bosch, E. Delp, D. Ebert, D. Kerr, and C. Boushey, "Evidence-based development of a mobile telephone food record," *Journal of American Dietetic Association*, vol. 110, pp. 74–79, January 2010.

[13] T. Schap, B. Six, E. Delp, D. Ebert, D. Kerr, and C. Boushey, "Adolescents in the united states can identify familiar foods at the time of consumption and when prompted with an image 14 h postprandial, but poorly estimate portions," *Public Health Nutrition*, vol. 1, no. 1, pp. 1–8.

[14] M. Bosch, F. Zhu, N. Khanna, C. Boushey, and E. Delp, "Combining global and local features for food identification and dietary assessment," *Proceedings of the International Conference on Image Processing (ICIP)*, Brussels, Belgium, 2011.

[15] F. Zhu, M. Bosch, and E. Delp, "An image analysis system for dietary assessment and evaluation," *Proceedings of the IEEE International Conference on Image Processing (ICIP)*, Hong Kong, China, September 2010.

[16] J. Chae, I. Woo, S. Kim, R. Maciejewski, F. Zhu, E. J. Delp, C. J. Boushey, and D. S. Ebert, "Volume estimation using food specific shape templates in mobile image-based dietary assessment," vol. 7873, no. 1. SPIE, January 2011, p. 78730K.

[17] Z. Zhang, "A flexible new technique for camera calibration," *IEEE Transactions on Pattern Analysis and Machine Intelligence*, vol. 22, no. 11, pp. 1330–1334, 2000.

[18] J. Bouguet, "Camera calibration toolbox for matlab," 2004.

[19] G. Bradski and A. Kaehler, *Learning OpenCV: Computer vision with the OpenCV library*. O'Reilly Media, 2008.

[20] M. Rufli, D. Scaramuzza, and R. Siegwart, "Automatic detection of checkerboards on blurred and distorted images," *IEEE/RSJ International Conference on Intelligent Robots and System*. IEEE, 2008, pp. 3121–3126.

[21] Z. Wang, Z. Wang, and Y. Wu, "Recognition of corners of planar pattern image," *World Congress on Intelligent Control and Automation (WCICA)*, July 2010, pp. 6342 –6346.

[22] A. de la Escalera and J. M. Armingol, "Automatic Chessboard Detection for Intrinsic and Extrinsic Camera Parameter Calibration," *Sensors*, vol. 10, no. 3, pp. 2027–2044, March 2010.

[23] V. N. Dao and M. Sugimoto, "A Robust Recognition Technique for Dense Checkerboard Patterns," *International Conference on Pattern Recognition*, pp. 3081–3084, Aug. 2010.

[24] W. Sun, X. Yang, S. Xiao, and W. Hu, "Robust checkerboard recognition for efficient nonplanar geometry registration in projector-camera systems," *Proceedings of ACM/IEEE International Workshop on Projector camera systems (PROCAMS)*, vol. 1, no. 212, New York, New York, USA, 2008, pp. 2.1–2.7.

[25] V. Vezhnevets, "OpenCV calibration object detection," 2005.

[26] D. Douglas and T. Peucker, "Algorithms for the reduction of the number of points required to represent a digitized line or its caricature," *Cartographica: The International Journal for Geographic Information and Geovisualization*, vol. 10, no. 2, pp. 112–122, 1973.

[27] D. Lowe, "Distinctive image features from scale-invariant keypoints," *International Journal of Computer Vision*, vol. 2, no. 60, pp. 91–110, 2004.

[28] N. Joshi, S. Kang, C. Zitnick, and R. Szeliski, "Image deblurring using inertial measurement sensors," *ACM Transactions on Graphics (TOG)*, vol. 29, no. 4, pp. 1–9, 2010.

[29] L. Yuan, J. Sun, L. Quan, and H.-Y. Shum, "Image deblurring with blurred/noisy image pairs," *ACM Transactions on Graphics*, vol. 26, July 2007.

[30] Q. Shan, J. Jia, and A. Agarwala, "High-quality motion deblurring from a single image," *ACM Trans. Graph.*, vol. 27, pp. 73:1–73:10, August 2008.

[31] X. Marichal, W. Ma, and H. Zhang, "Blur determination in the compressed domain using dct information," *IEEE International Conference on Image Processing*, vol. 2, 1999, pp. 386–390.

[32] P. Marziliano, F. Dufaux, S. Winkler, and T. Ebrahimi, "Perceptual blur and ringing metrics: application to JPEG2000," *Signal Processing and Image Communication*, vol. 19, no. 2, pp. 163–172, 2004.

[33] N. Narvekar and L. Karam, "A No-Reference Image Blur Metric Based on the Cumulative Probability of Blur Detection (CPBD)," *IEEE Transactions on Image Processing*, vol. PP, no. 99, p. 1, 2011.